



REVIEW ARTICLE

# Intravascular hemodynamics and coronary artery disease: New insights and clinical implications



CrossMark

Marina Zaromytidou <sup>a</sup>, Gerasimos Siasos <sup>a</sup>, Ahmet U. Coskun <sup>b</sup>,  
Michelle Lucier <sup>a</sup>, Antonios P. Antoniadis <sup>a</sup>,  
Michail I. Papafaklis <sup>a</sup>, Konstantinos C. Koskinas <sup>a</sup>,  
Ioannis Andreou <sup>a</sup>, Charles L. Feldman <sup>a</sup>, Peter H. Stone <sup>a,\*</sup>

<sup>a</sup> Cardiovascular Division, Brigham and Women's Hospital, Harvard Medical School, Boston, MA, United States

<sup>b</sup> Mechanical and Industrial Engineering, Northeastern University, Boston, MA, United States

Received 15 December 2015; accepted 26 July 2016

Available online 25 November 2016

## KEYWORDS

Endothelial shear stress;  
Atherosclerosis;  
Acute coronary syndromes

**Abstract** Intracoronary hemodynamics play a pivotal role in the initiation and progression of the atherosclerotic process. Low pro-inflammatory endothelial shear stress impacts vascular physiology and leads to the occurrence of coronary artery disease and its implications.

© 2016 Hellenic Society of Cardiology. Publishing services by Elsevier B.V. This is an open access article under the CC BY-NC-ND license (<http://creativecommons.org/licenses/by-nc-nd/4.0/>).

## 1. Introduction

The field of cardiovascular disease has experienced enormous progress, but atherosclerotic coronary artery disease (CAD) remains the leading cause of death. Atherosclerosis is

characterized by an early onset with a long interval before clinical symptoms appear as well as heterogeneity in its phenotypic expression and natural history. The identification and control of coronary risk factors, such as diabetes, smoking, arterial hypertension and hyperlipidemia, is the cornerstone of preventative strategies.<sup>1</sup> Atherosclerotic lesions tend to form at certain arterial segments (e.g., branch points, curvatures, bifurcations, downstream of an obstruction) despite the systemic effect of risk factors on the vasculature, and only a small percentage of coronary lesions lead to a clinical event. Therefore, local factors must determine the localization and progression of the atherosclerotic process. Extensive in-vitro and in-vivo

\* Corresponding author. Peter H. Stone, Cardiovascular Division, Brigham and Women's Hospital, 75 Francis St, Boston, MA 02115, United States. Tel.: +1 8573071965; fax: +1 8573071955.

E-mail address: [pstone@partners.org](mailto:pstone@partners.org) (P.H. Stone).

Peer review under responsibility of Hellenic Society of Cardiology.

studies concluded that intracoronary hemodynamics and particularly flow-derived endothelial shear stress (ESS) are the most prominent factors that underlie the diversity of the natural history of atherosclerosis in susceptible individuals with CAD risk factors.

## 2. Hemodynamic factors affecting blood vessels

### 2.1. Mechanical forces

Blood circulates through the vasculature following the cardiac cycle. Vessel geometry alters the hemodynamic characteristics, and changes in blood flow affect the morphology and function of arteries. This constant interaction between blood flow and arterial geometry results in the production of a complex hemodynamic pattern with varying spatio-temporal characteristics.<sup>2–4</sup>

The metric used to quantify the biomechanical forces induced by blood pressure and flow is called stress, and it is defined as a force normalized by the area to which the force is applied. Blood pressure-derived force, known as tensile stress (TS), is distributed circumferentially to the arterial wall, and it is represented by the Laplace's law equation ( $TS = P(r/h)$ , where  $P$  is mean arterial blood pressure,  $r$  is the lumen radius and  $h$  is vessel wall thickness). Blood flow also produces tangential forces,<sup>5,6</sup> which is the friction of the flowing blood on the endothelial surface, called endothelial shear stress (ESS), which is proportional to the product of blood viscosity ( $\mu$ ) and the spatial gradient of blood velocity at the wall ( $ESS = \mu \times dv/dy$ ) (Fig. 1). The arterial wall properties and structure (arterial stiffness) also modify the impact of TS and ESS on the lumen.<sup>7</sup>

Coronary blood flow, blood properties (primarily viscosity) and arterial geometry determine the characteristics of ESS. Laminar blood flow is characterized as smooth and streamlined, and it is further categorized into disturbed or undisturbed flow according to the presence or absence of reverse flow, respectively.<sup>8,9</sup> Arterial geometry determines the ESS pattern formed. The presence of bifurcations, branches, curves and obstructions modifies flow and ESS

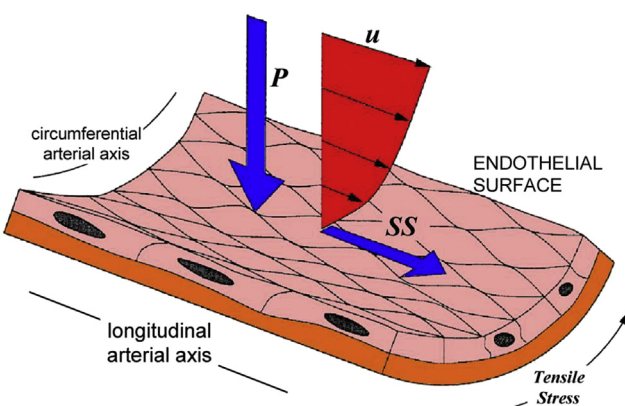


**Figure 1** Mechanical forces that impact the arterial wall. SS = shear stress, P = arterial pressure, u = blood velocity.

patterns.<sup>10</sup> Blood flow enters these lower pressure regions and generates flow separation, recirculation and reattachment zones (reverse flow), which is characterized as low ESS (Fig. 2a). These disturbed flow zones are also encountered upstream and downstream of obstructions, such as stenotic atherosclerotic plaques, at stented lesions and at coronary artery-vein graft junctions after a coronary bypass surgery.<sup>11</sup>

Therefore, the complex interactions of blood flow, viscosity and arterial geometry generate the different ESS patterns that are characterized by their direction (unidirectional, bidirectional) and magnitude (low, moderate, high). Moderate ESS varies between 1.5 -3.0 Pa over the cardiac cycle, and it is encountered in relatively straight arterial segments, where it exhibits unidirectional flow with atheroprotective effects. High ESS refers to values over 3 Pa, which is present at the stenotic site of atherosclerotic plaques. Low ESS (below 1-1.5 Pa) with undisturbed unidirectional flow occurs at the inner areas of curvatures and upstream of stenosis.<sup>12,13</sup> Low oscillatory ESS is characterized by bidirectional flow (reverse flow), and it is observed at the ostia of branches, downstream of stenotic plaques and at the lateral walls of bifurcations (Fig. 2b). Low and/or oscillatory ESS promotes pro-atherogenic pathways, and it is a key factor in the development and progression of focal atherosclerosis.<sup>13,14</sup>

### 2.2. ESS and atherosclerosis

Atherosclerosis is a complex disease that involves various components of normal arteries, such as endothelial cells, smooth muscle cells (SMC) and arterial extracellular matrix macromolecules, which undergo a phenotypic switch from their normal physiological function under the stimulation of local flow hemodynamics and inflammatory mechanisms. There are several key points of the atherosclerotic process. (1) The transportation, subendothelium accumulation/retention and modification of low density lipoprotein (LDL) particles that trigger the inflammatory cascade, activate endothelial cells and signal the recruitment and migration of monocytes into the endothelium. (2) The subsequent differentiation of monocytes into macrophages that facilitates the phagocytosis of modified LDL and form foam cells that amplify the inflammatory micro-environment, which gradually progress into atherosclerotic lesions. (3) The migration and differentiation of smooth muscle cells (SMCs) to the intima that participating in all atherosclerotic stages by altering extracellular matrix synthesis and releasing cytokines and adhesion molecules involved in monocyte recruitment and macrophage proliferation.<sup>15</sup> Endothelial shear stress is implicated in the regulation of all of these critical steps, which supports its important role in atherosclerosis initiation and progression.

#### 2.2.1. Mechanosensing and mechanotransduction

The endothelium plays a crucial role in the initiation and progression stages of atherosclerosis because it is the barrier between blood flow and arterial layers. Normal endothelial cells sense changes in the microenvironment and regulate important functions, such as vascular tone, circulating cell adhesion, coagulation, fibrinolysis, and vessel wall inflammation, in response to hemodynamic

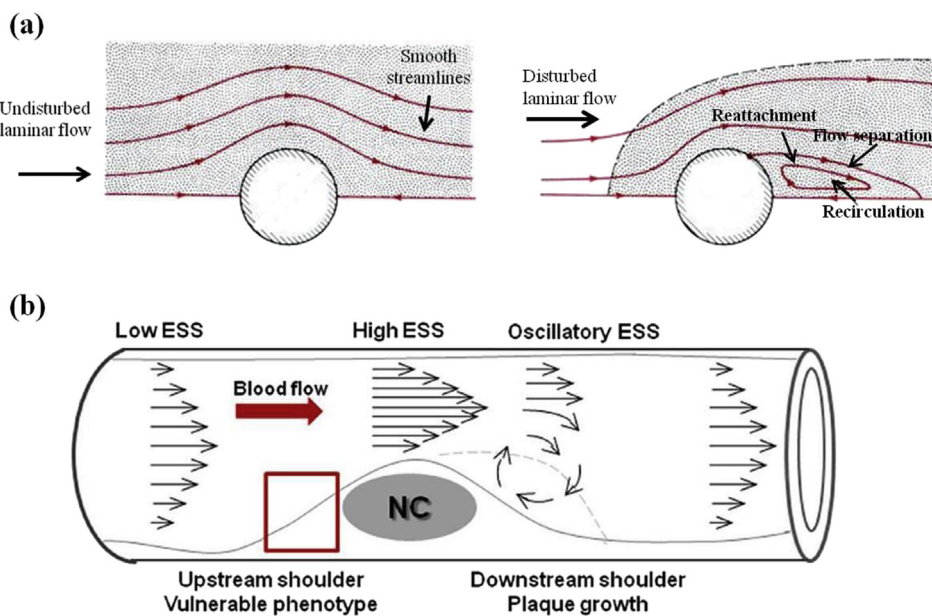


**Figure 2** (a) Types of blood flow, (b) distribution of ESS patterns along the length of an atherosclerotic lesion. NC = necrotic core.

changes. Endothelial cells are arranged in a specific manner on the artery surface to form a tight seal, which controls the transportation of all molecules between the lumen and intima.

The identification of the different flow patterns (mechanosensing) is mediated by numerous endothelial mechanosensors, including ion channels, G-proteins, caveolae, tyrosine kinase receptors, nicotinamide adenine dinucleotide phosphate (NADPH), adhesion molecules (PECAM-1/ VE-cadherin/ VEGFR2), primary cilium, integrins, glycocalyx and the actin cytoskeleton. The detection of shear stress stimuli leads to the physical deformation of the cell surface, intracellular signal transmission and conversion of the mechanical force into the chemical molecules that generate the endothelial response via differential gene expression (mechanotransduction).<sup>16,17</sup> Laminar flow and unidirectional high shear stress create an atheroprotective endothelial phenotype, and low/ oscillatory ESS is responsible for a proatherogenic phenotype. Different ESS patterns exert their gene modulation via the anti-inflammatory transcription factor (TF) Kruppel-like factor 2 (KLF2) and the proinflammatory nuclear factor- $\kappa$ B (NF- $\kappa$ B).<sup>18,19</sup> The complex, partially understood mechanisms of mechanosensing, mechanotransduction and gene regulation translate the ESS stimuli and drive the endothelium to respond by altering its cell conformation, permeability and production of atheroprotective and proatherogenic molecules.

Endothelial cell (EC) orientation and structure is modified according to blood flow types. Specifically, ECs exposed to high ESS are elongated and aligned with laminar flow, but low/oscillatory ESS leads to poorly aligned cells with structural changes from fusiform to polygonal shapes. The mitotic and endothelial apoptotic cell cycles are attenuated in low/oscillatory ESS sites, which results in the widening of cell-to-cell junctions, increases the

permeability of endothelial surface and facilitates the infiltration of molecules.<sup>20</sup>

Stimuli for LDL internalization include the presence of hyperlipidemia in combination with ESS-induced increased endothelium permeability, the ESS-upregulated expression of genes encoding for the LDL receptor of the endothelial membrane, and the prolonged residence time of LDL particles near the endothelium due to low and oscillatory ESS.<sup>13,21,22</sup> Certain stimuli, including low ESS, signal the migration of VSMCs from the media to the intima tunica, where these cells proliferate and produce proteoglycans that contribute to LDL retention, intimal thickening and fibrous cap formation.<sup>9,23</sup> Low ESS reverses the endothelial microenvironment in favor of monocyte adherence and migration by triggering the expression of adhesion molecules on the endothelial cell membrane and the secretion of chemoattractant cytokines to initiate the inflammatory cascade.<sup>24</sup>

Retention of LDL results in its oxidation by reactive oxygen species (ROS), which is upregulated in sites of low ESS and augments inflammatory pathways (e.g., production of inflammatory cytokines and adhesion molecules) and endothelial dysfunction and triggers the differentiation of monocytes into macrophages that encapsulate oxidized LDL and form foam cells.<sup>25</sup> ROS reduces the availability of NO, which minimizes its anti-thrombotic, anti-mitogenic and anti-inflammatory properties (e.g., prevention of LDL oxidation and monocyte adhesion/transmigration into the intima). Activation of endothelial nitric oxide synthase (eNOS) only occurs in areas with physiological ESS, which deprives regions with disturbed flow of the atheroprotective effects of NO.<sup>26,27</sup>

Vessel architecture is altered during atherosclerosis progression, which leads to vascular remodeling. Low ESS triggers the infiltration of macrophages into the subendothelium-accumulated lipoproteins, which forms

the necrotic lipid core that gradually grows in size and inevitably disturbs arterial structure and geometry. The production of extracellular matrix (ECM) molecules (e.g., collagen and elastin) from VSMCs and fibroblasts is normally counterbalanced by the activity of matrix-degrading enzymes, primarily metalloproteinases (MMPs) and cathepsins, which maintain the integrity of the arterial wall. The balance between ECM synthesis and degradation is dysregulated in a low ESS milieu, which alters the arterial architecture. The expression and activity of MMPs and cathepsins is enhanced as dysfunctional endothelial cells upregulate MMP and cathepsin gene expression.<sup>28</sup> The accumulation and activation of macrophages and VSMCs by pro-inflammatory cytokines increases MMP release.<sup>29</sup> Low ESS interferes with VSMC function by promoting the expression of growth factors that trigger the migration, differentiation and proliferation of VSMCs and pro-inflammatory cytokines, which halts ECM production and signals VSMC apoptosis (Fig. 3).<sup>13</sup> ESS also modifies the arterial structure by promoting neovascularization (e.g., the upregulation of VEGF and other angiogenic stimuli) and intraplaque hemorrhage.<sup>28,30,31</sup>

### 2.3. ESS and manifestations of coronary atherosclerosis

Biomechanical factors substantially contribute to the formation of vulnerable plaques and the actual event of plaque rupture or erosion.<sup>6,32</sup> Atherosclerotic plaques are formed by a lipid-rich necrotic core and a fibrous cap that separates the core from the vessel lumen, which averts the contact of the thrombogenic core compounds with blood flow. Ruptured plaques are characterized by a weakened fibrous cap that is susceptible to mechanical hemodynamic

forces, mostly tensile stress. The collagen concentration is crucial for the fibrous cap to withstand these forces. The increased proteolytic MMP function and decreased SMC collagen synthesis in sites of low ESS may account for the fibrous cap thinning that predisposes it to plaque rupture. The excessive and expansive remodeling of the plaque in sites of low ESS and intense MMP activity are associated with plaque vulnerability.<sup>29,33,34</sup> A large necrotic core is associated with plaque rupture because of the anatomical-mechanical changes it provokes and increased macrophage infiltration are evident in rupture-prone plaques.<sup>35</sup>

The mechanisms responsible for plaque erosion are not as well studied as the mechanisms responsible for plaque rupture. Most of the erosions occur downstream of plaques, where sites are typically subjected to low ESS. Low ESS regions are characterized by increased endothelial cell turnover, endothelial cell apoptosis and impairment of the endothelial glycocalyx, which ultimately results in endothelial denudation. Consequently, low ESS is involved in the pathogenetic mechanism of erosion.<sup>20,36,37</sup>

The thrombogenic material of the necrotic core is exposed to the bloodstream after rupture or erosion, which results in thrombus formation that partially/totally occludes the lumen or remains contained in the vascular wall. The factors that determine the impact of thrombus on the vessel include the magnitude of the plaque cap disruption and the blood thrombogenicity, which is increased in sites with abnormal ESS values.<sup>38,39</sup>

### 3. In vivo techniques to investigate local ESS

The detrimental role of ESS in the initiation and progression of atherosclerosis emphasizes the need for a validated tool to assess ESS values in humans. ESS patterns depend on

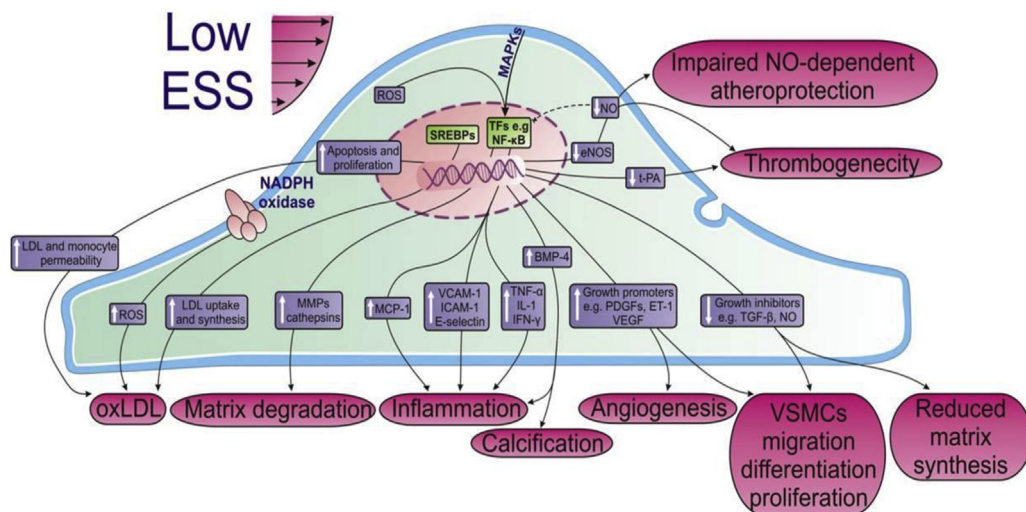


**Figure 3** Endothelial cells in a low ESS milieu signal the initiation and progression of the atherosclerotic process by affecting important functions, such as vascular tone, circulating cell adhesion, coagulation, fibrinolysis and vessel wall inflammation. LDL = low density lipoprotein, ROS = reactive oxygen species, MMPs = matrix metalloproteinases, MCP = monocyte chemoattractant protein, VCAM = vascular cell adhesion molecule, ICAM = intercellular adhesion molecule, TNF = tumor necrosis factor, IL = interleukin, IFN = interferon, BMP = bone morphogenic protein, PDGF = platelet-derived growth factor, VEGF = vascular endothelial growth factor, ET = endothelin, TGF = transforming growth factor, NO = nitric oxide, t-PA = tissue plasminogen activator, VSMCs = vascular smooth muscle cells, SREBP = sterol regulatory elements binding protein, TFs = transcription factors, NF-κB = nuclear factor kappa-light-chain-enhancer of activated B cells.

coronary artery geometry and blood flow type, and an accurate 3D reconstruction of the vessel geometry and coronary blood flow values is a prerequisite for estimating ESS. These particular data are derived using invasive imaging modalities, such as intravascular ultrasound (IVUS) and optical coherence tomography (OCT) after fusion with coronary angiography, and noninvasive imaging tools, such as coronary computed tomography angiography (CCTA).

The technology used to assess ESS has evolved tremendously during the last decade. Assessments of ESS are not performed in real time and require the transfer of imaging data to laboratories with proper equipment and expertise, but these factors are expected to change in the near future.

### 3.1. Invasive techniques

The 3D reconstruction of the coronary artery after acquisition of IVUS or OCT and x-ray angiography data are the gold standards in ESS assessment because these techniques are standardized and validated. Coronary angiography produces a 2D outline of the arterial lumen throughout its course on the epicardial surface that is not adequate for 3D reconstruction without the addition of additional more

precise imaging modalities of the arterial wall and lumen. Two angiographic images obtained from orthogonal views are selected that correspond to the same coronary segments with the IVUS or OCT pullback. The lumen and EEM borders are traced in each IVUS or OCT frame to facilitate the extraction of the basic geometrical characteristics of the vessel, which are subsequently oriented in 3D space according to the angiographic information.<sup>40</sup> The methodology for ESS assessments required pre-planned protocols that utilize the IVUS catheter path to provide an accurate orientation for the 3D model until recently. The introduction of the centerline method, which generates the 3D reconstruction with the implementation of data derived from routine coronary angiography and IVUS, simplifies the procedure and allows the retrospective ESS interrogation of imaging data banks.<sup>41</sup>

The second step in ESS assessment methods is the calculation of coronary blood flow to the reconstructed 3D artery. Coronary blood flow in the arterial section (a section free of significant side branches that may alter the flow) is calculated from the time required for the volume of blood contained within the section to be displaced by radio-opaque material during a contrast injection or via the use of Doppler velocity measurements (Fig. 4).<sup>40,42,43</sup>

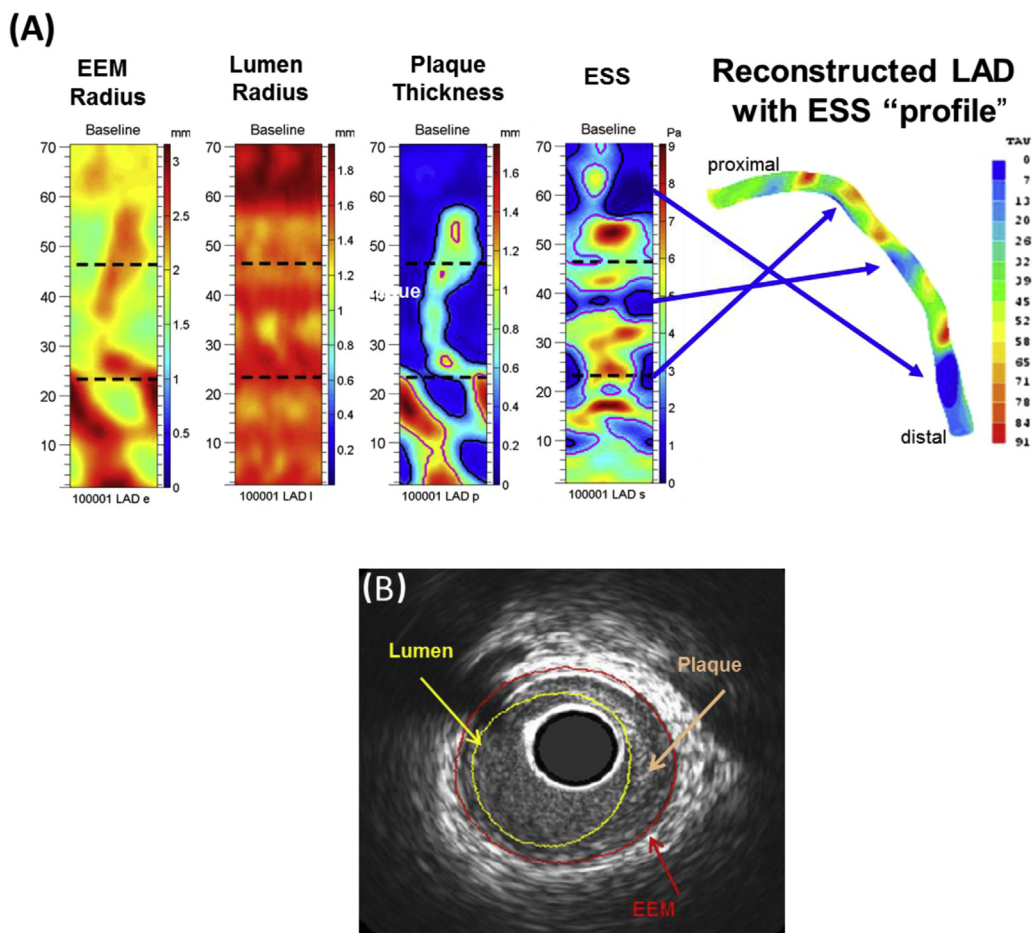


**Figure 4** (A) Cross sectional OCT image with implemented local ESS values (lumen border), (B) Cross sectional IVUS image and (C) Example of ESS and LAD coronary wall morphology after the 3D reconstruction and computational fluid dynamics. EEM = external elastic membrane, ESS = endothelial shear stress, LAD = left anterior descending, Pa = Pascal.

In an effort to further simplify ESS assessment, 3D artery reconstruction may be generated using only information from biplane angiography, a technique known as 3D quantitative coronary angiography (3D QCA).<sup>44,45</sup> Although 3D QCA is suggested as a less time-consuming and complicated method, major drawbacks exist. Lumen area and vessel diameter detection is far inferior to IVUS or OCT precision, and the lack of its ability to provide information about plaque components and vascular remodeling restricts its use in ESS assessments.<sup>46,47</sup>

IVUS and OCT provide ESS assessments and plaque characterization, but novel imaging modalities, such as near-infrared spectroscopy (NIRS) / near-infrared fluorescence (NIRF), provide valuable information of plaque composition and the possible role of inflammation.

### 3.1.1. Intravascular ultrasound

Intravascular ultrasound is an invasive modality that produces images of the arterial lumen and wall by converting the reflected ultrasound waves into electrical signals. Its axial resolution (70 to 200  $\mu\text{m}$ ) and penetration ( $>5$  mm) enables the evaluation of lumen dimensions, arterial remodeling and PB that, combined with its good reproducibility, supports IVUS as an effective modality for investigations of the natural history of atherosclerotic disease. Certain limitations, such as the acoustic shadowing in calcified plaques and the inability to characterize plaque tissue components, led to the development of new techniques, such as virtual histology IVUS (VH-IVUS) and OCT, to address these issues. Virtual histology translates the IVUS radiofrequency backscatter signal into tissue color images (with each color signifying a precise tissue component), which supplements the gray scale (IVUS) images and amplifies the available information. VH-IVUS exhibits excellent predictive accuracies compared to histopathology samples, but several studies in porcine models questioned its reliable accuracy.<sup>48,49</sup>

### 3.1.2. Optical coherence tomography

Optical coherence tomography is an invasive imaging modality that generates cross-sectional images of the coronary vessel using the reflections of near-infrared light. The higher resolution (10-20  $\mu\text{m}$ ) of OCT compared to IVUS is used to depict structures that are otherwise not well characterized in IVUS images, such as thin fibrous cap, thrombus and endothelial coverage of stent struts. OCT was recently validated as a reliable modality for 3D coronary artery reconstruction and assessment of ESS values because of the more detailed and accurate imaging of coronary vessels, including vulnerable plaques and intracoronary devices. However, the inferior penetration depth of OCT compared to IVUS into the arterial wall provides information only for the superficial arterial layers and cannot evaluate vascular remodeling or plaque burden (PB).<sup>46,50,51</sup>

### 3.1.3. Novel imaging modalities

IVUS and OCT are valuable imaging modalities for the estimation of ESS and its association with the natural history of atherosclerosis. A hybrid IVUS-OCT catheter that combines the imaging depth of IVUS with the high resolution of OCT has been developed and tested ex vivo with promising results that await validation in human studies.<sup>52</sup>

The combination of IVUS or OCT with the techniques of near-infrared spectroscopy (NIRS) / near-infrared fluorescence (NIRF) also improves their imaging properties. Specifically, NIRS detects lipid core-containing plaques based on the absorption and scatter patterns of near-infrared light by the different plaque components.<sup>53-56</sup> The addition of NIRS to IVUS/OCT catheters enhances the characterization of plaque tissue regarding the lipid content, but the limited penetration of NIRS (1-2 mm) is inadequate for the study of deeper artery segments.<sup>53,57</sup> The implementation of NIRF in invasive intracoronary plaque assessment enables the study of the atherosclerotic mechanisms on a cellular/molecular level and provides information on inflammatory activity.<sup>58</sup> Animal and ex vivo studies support the introduction of NIRF to IVUS/OCT catheters as a promising tool for the evaluation of the natural history of atherosclerosis, but further technical improvements are warranted to allow testing in human studies.<sup>59-61</sup>

## 3.2. Non-invasive techniques

CCTA has been used to reconstruct the 3D geometrical model of the coronary artery for subsequent CFD analysis and ESS calculations in an effort to minimize invasive procedures and simplify the assessment of hemodynamic parameters.<sup>62,63</sup> A limited number of published data exist on the estimation of ESS and plaque morphology using CCTA, but the reported results are encouraging.<sup>64-66</sup> The non-invasive methodology of CCTA in ESS calculation avoids the complications that accompany the intracoronary techniques and allows CCTA to be performed in low and intermediate risk groups. However, the spatial resolution ( $\approx 400$   $\mu\text{m}$ ) of CCTA cannot visualize small diameter branches ( $<0.5$  mm) or accurately identify certain plaque or arterial wall characteristics and subtle changes in atherosclerotic morphology, and the presence of calcifications obscures lumen borders.<sup>67-70</sup> Commercial software for the quantification of PB exhibits good intra-platform reproducibility, but industry standards should be applied to overcome the poor interplatform reproducibility.<sup>71</sup>

## 4. Role of ESS in the natural history of atherosclerosis

The development of effective evaluation techniques utilizing well validated and routinely used imaging modalities paved the way for the in-vivo study of ESS in animal models and humans. Understanding the role of ESS in CAD progression may be best accomplished with studies that are designed to evaluate the ESS values and vessel morphology in serial time points.

### 4.1. Animal studies

Animal studies to evaluate the natural history of atherosclerosis using ESS were performed in hypercholesterolemic swine models because of the characteristic development of human-like advanced atherosclerotic plaques. Animal studies provide significant advantages of histopathological analyses, which are the gold standard in plaque tissue

characterization, immunostaining and gene expression measurement.

The results from the swine models support the detrimental role of low ESS in the initiation and progression of atherosclerosis in the presence of systemic risk factors (hyperlipidemia, hyperglycemia). Chatzizisis et al. demonstrated that low ESS sites were associated with intense subendothelium lipid accumulation, inflammation, severe internal elastic lamina degradation, excessive expansive remodeling and fibrous cap thinning.<sup>4</sup> Koskinas et al. examined the interaction between ESS and vascular remodeling in a natural history study consisting of 5 time points and provided new insights that low ESS was associated with the early initiation and the ongoing progression of focal plaques. Vascular remodeling was a highly dynamic, temporally changing response to local plaque formation. Marked heterogeneity of remodeling patterns at each time point was reported, and compensatory expansive remodeling was identified as the predominant vascular response. Individual plaques also exhibit a heterogeneous course that evolves through a variety of remodeling patterns throughout their natural history while local ESS values adapt to changes in vessel lumen and dimensions. Regions of very low ESS resulted in plaques with excessive expansive remodeling, which further exacerbated the low ESS environment and augmented subsequent plaque progression. Conversely, lesions with compensatory or constrictive remodeling were characterized by an amelioration of the adverse low ESS stimulus and a trend towards less marked further growth. A small subpopulation of coronary segments was exposed to a progressively worsening stimulus of low ESS throughout their evolution, and these segments ultimately evolved to presumed highest-risk plaques. These high-risk lesions were identified in-vivo at earlier stages of their natural history using the combined assessment of local ESS, plaque thickness and vascular remodeling.<sup>34</sup>

Arterial regions exposed to low ESS exhibited reduced endothelial cell coverage, augmented infiltration of activated inflammatory cells, and substantially increased expression and enzymatic activity of elastolytic MMPs relative to their inhibitors. These enzymes likely contribute to the fragmentation of elastin fibers and promote the excessive expansive remodeling response of the vessel wall, which ultimately promotes the formation of atheromata with thin fibrous caps.<sup>33</sup> A similar serial study from a different animal cohort complements the former results by emphasizing the association of local low ESS with the formation of lesions with reduced SMC content and augmented expression and activity of collagenases, which favors attenuated synthesis and increased catabolism of collagen. This imbalance likely contributes to the evolution of early lesions to collagen-poor, thin-capped atheromata.<sup>29,72</sup>

A recent study examined the association of ESS with atherosclerotic initiation and progression by placing a stenotic shear modifying stent (SMS) in the coronary arteries of mini-pigs and assessing ESS values using OCT. The results supported previously published data of the presence of low and multidirectional ESS downstream of SMS and associating these factors with plaque progression and TCFA phenotype.<sup>67</sup>

Local and systemic factors must coexist for atherosclerosis to initiate and progress, but the nature of their interaction was not investigated until quite recently. Koskinas et al. demonstrated that the pro-atherogenic threshold of low ESS was cholesterol-dependent, with increasing cholesterol levels exaggerating low ESS effects and diminishing the atheroprotective effects of higher ESS.<sup>73</sup> The results of the animal studies support ESS as a key factor in the mechanisms of atherosclerosis and highlight the importance of local hemodynamic conditions in the setting of systemic risk factors.

## 4.2. Human studies

### 4.2.1. Natural History of CAD

The first human studies were published approximately a decade ago and demonstrated that ESS was a significant determinant of atherosclerotic plaque progression and vascular remodeling. Stone et al. reported that plaque progression occurred almost exclusively in areas of low ESS and may be accompanied by expansive or constrictive remodeling.<sup>74,75</sup> Subsequent studies by Samady et al. also support the role of ESS in CAD associating low ESS with plaque progression.<sup>76–78</sup>

These studies substantially contributed to elucidating the role of ESS in atherosclerosis, but they are limited by the small population number. The Prediction of Progression of Coronary Artery Disease and Clinical Outcomes Using Vascular Profiling of Shear Stress and Wall Morphology (PREDICTION) Study was the largest serial anatomical natural history study of coronary atherosclerosis conducted in 506 Japanese patients who presented with an acute coronary syndrome and underwent percutaneous coronary intervention (PCI) at the culprit lesion followed by 3 vessel imaging with IVUS and angiography. The positive predictive value to predict clinically relevant obstruction progression treated with PCI of baseline PB was estimated as 22% but rose to 41% when the baseline pro-inflammatory low ESS was considered. Further analyses, which included IVUS-based tissue characteristics, revealed that the highest positive predictive value (53%) and diagnostic accuracy (88%) were demonstrated when low ESS and large necrotic content were present. The negative predictive value remained high (91%) if all predictors were absent (Fig. 5).<sup>79</sup> Baseline low ESS was an independent predictor of plaque progression and worsening luminal obstruction in routine natural history of CAD and the development of clinically relevant lesions treated with PCI. No association between high ESS and plaque progression was observed. Very few clinical events occurred in this low-risk Japanese patient population. Therefore, an association between baseline vascular characteristics and subsequent major adverse clinical events could not be studied.<sup>80,81</sup>

The Providing Regional Observations to Study Predictors of Events in the Coronary Tree (PROSPECT) study was a natural history study of coronary atherosclerosis conducted in 697 patients who presented with ACS in America and Europe and were followed for a median period of 3.4 years. This study provided an opportunity to examine the role of low ESS in plaque progression in a truly high-risk population. The non-culprit lesions associated with subsequent

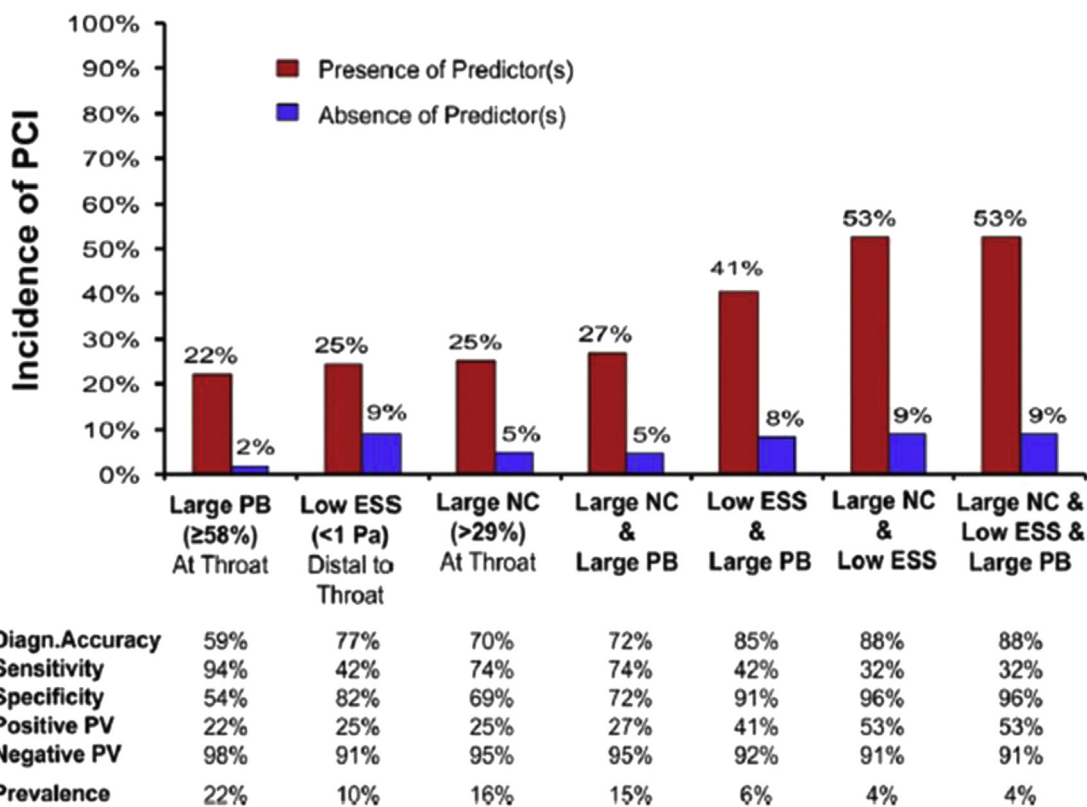


**Figure 5** Incidence of PCI for symptoms or plaque progression according to independent predictors- The PREDICTION study. PB = plaque burden, ESS = endothelial shear stress, NC = necrotic core, PCI = percutaneous coronary intervention, PV = predictive value.

major adverse cardiovascular events were characterized at baseline by a large PB ( $\geq 70\%$ ), small minimal luminal area ( $\leq 4.0 \text{ mm}^2$ ) and the appearance of TCFA by radiofrequency IVUS. The hazard ratio for major adverse cardiovascular events at 3 years was high (11.05) if all 3 lesion characteristics were present at baseline.<sup>82</sup> Stone et al. investigated the incremental prognostic role of low ESS in a post-hoc analysis of the PROSPECT study to predict new MACE and the anatomic characteristics in the high-risk Western population of the PROSPECT study. The preliminary results demonstrated that the presence of local low ESS within a lesion provides substantial incremental prognostication for future major adverse events when added to the other known prognostic anatomic characteristics, an observation highlighted by the fact that there were no MACE outcomes in follow-up if the lesion did not exhibit local low ESS at baseline regardless of PB, MLA, or lesion phenotype at baseline.<sup>83</sup>

Recent serial natural history studies indicate that most plaques also exhibit a highly variable natural history. Most plaques, even advanced plaques, become quiescent over time, but other plaques may evolve to become more highly inflamed and more prone to rupture.<sup>34,84</sup> The observation in PROSPECT that  $<4\%$  of large PB lesions and  $<5\%$  of TCFA histology lesions were associated with a new MACE support the concept that the majority of even ostensibly high-risk plaques generally become quiescent. In contrast, a non-culprit lesion that remains in a low ESS microenvironment will likely continue to progress whether it appears to be a

TCFA or a ThCFA at the single baseline anatomical "snapshot" of imaging during the index culprit lesion event.

The recent implementation of high-resolution OCT in ESS computation provides more detailed information on plaque characteristics with respect to ESS value. One study in patients presenting with ACS used OCT and identified low ESS areas that exhibited larger lipid accumulation, higher prevalence of spotty calcification and macrophage density compared to higher ESS regions. One interesting finding was that low ESS plaques displayed thinner fibrous caps, and the TCFA phenotype was present almost exclusively in low ESS plaques, which confirms previous results from animal studies. However, only a small percentage of low ESS lesions presented a TCFA phenotype, which suggests that a multifactorial pattern defines plaque characteristics, in which ESS plays a significant role. Notably, this study investigated ESS and plaque morphology only at one time point, and the variability in the natural history of individual plaques was not evaluated.<sup>85</sup>

#### 4.2.2. Role of Local ESS in Outcomes following Stent Deployment

Several human studies focused on ESS assessment in interventional cardiology and stent deployment. Neointimal formation, neoatherosclerosis and in-stent restenosis are the nemeses of interventional cardiologists. ESS was recently investigated as a parameter affecting prognosis after stent implantation. Stent placement injures the endothelium and arterial wall, which alters the local

geometry and blood flow (flow separation, recirculation).<sup>86</sup> The development and implementation of drug-eluting stents significantly reduced the formation of neointimal hyperplasia compared to bare metal stents. Several studies support the notion that ESS drives in-stent neointimal hyperplasia/ neoatherosclerosis and contributes to stent failure, which stimulated the search for optimal stent position strategy and structure.<sup>87–89</sup> ESS does not seem to affect the arterial wall behind the struts, perhaps because of the altered compressed arterial structure.<sup>87, 90</sup> One recent study stressed the importance of hemodynamic factors in the neointimal response after Absorb bioresorbable vascular scaffold implantation, which motivates studies for a more ergonomic stent design.<sup>87</sup> The same study group suggested that the interrogation of a stented artery in terms of ESS should be performed with the fusion of OCT and angiography because it is superior to IVUS/angiography fusion.<sup>91</sup>

Important studies, such as PROSPECT and PREDICTION, provided significant data on the natural history of atherosclerosis and validated results of smaller studies, but pieces of the puzzle remain missing. The design of large human studies that prospectively investigate the role of ESS in atherosclerosis using imaging modalities with improved resolution and penetration of plaque/tissue characterization (e.g., IVUS/NIRS, OCT/IVUS, OCT/NIRF) would further elucidate the pathophysiological mechanisms of CAD.<sup>92</sup>

## 5. Future plans/directions

Coronary hemodynamics and ESS are major determinants of the natural history of atherosclerosis. The role of ESS in the initiation of endothelial dysfunction, atherosclerosis, vascular remodeling and plaque stability is well documented.

The identification of specific atherosclerotic plaques that are prone to rupture or erosion and cause adverse cardiovascular events is of the utmost importance. Early stent placement or local drug delivery to vulnerable plaques may prevent CAD complications. Unfortunately, the level of evidence available is not sufficient to accurately identify high-risk plaques. Studies that will fully elucidate the complex role of pro-inflammatory low ESS in the transition of plaques from a stable to vulnerable phenotype and translate the prognostic information in ESS mapping are warranted.

The illuminating of ESS mechanisms may also provide insights of the pleiotropic effects of various cardiovascular medications or offer new therapeutic approaches using drugs that target specific signaling pathways. Chronic administration of valsartan or valsartan/ simvastatin in animal models attenuates the proatherogenic effects of low ESS independent of their antihypertensive and hypolipidemic properties.<sup>93</sup> Widely prescribed cardiovascular regimens, such as statins and the β-blocker metoprolol, seem to exert atheroprotective effects via attenuation of the low ESS impact or restoration of atheroprotective ESS values, respectively.<sup>94,95</sup> However, the development of new mechano-sensitive drug containers that are activated by high shear stress to release the drug are being investigated to provide a more prompt and effective treatment of acute myocardial infarction and stroke.<sup>96</sup>

The techniques that are currently used to assess ESS are primarily invasive and relatively time-consuming, which restricts the study of ESS exclusively to the research field. The introduction of newer techniques that overcome these methodological limitations will allow a wider application and study of ESS, which will deliver an invaluable body of data and contribute enormously to an understanding of the detailed mechanisms responsible for plaque progression and ultimate disruption and inform new pre-emptive interventions.

## References

1. Laslett LJ, Alagona Jr P, Clark 3rd BA, et al. The worldwide environment of cardiovascular disease: prevalence, diagnosis, therapy, and policy issues: a report from the American College of Cardiology. *Journal of the American College of Cardiology*. 2012;60:S1–S49.
2. Malek AM, Alper SL, Izumo S. Hemodynamic shear stress and its role in atherosclerosis. *JAMA*. 1999;282:2035–2042.
3. Libby P. Inflammation in atherosclerosis. *Nature*. 2002;420: 868–874.
4. Chatzizisis YS, Jonas M, Coskun AU, et al. Prediction of the localization of high-risk coronary atherosclerotic plaques on the basis of low endothelial shear stress: an intravascular ultrasound and histopathology natural history study. *Circulation*. 2008;117:993–1002.
5. Steinman DA. Simulated pathline visualization of computed periodic blood flow patterns. *J Biomech*. 2000;33:623–628.
6. Kwak BR, Back M, Bochaton-Piallat ML, et al. Biomechanical factors in atherosclerosis: mechanisms and clinical implications. *Eur Heart J*. 2014;35:3013–3020, 20a–20d.
7. Papaioannou TG, Stefanidis C. Vascular wall shear stress: basic principles and methods. *Hellenic J Cardiol*. 2005;46:9–15.
8. Giannoglou GD, Chatzizisis YS, Zamboulis C, Parcharidis GE, Mikhailidis DP, Louridas GE. Elevated heart rate and atherosclerosis: an overview of the pathogenetic mechanisms. *Int J Cardiol*. 2008;126:302–312.
9. Tarbell JM, Shi ZD, Dunn J, Jo H. Fluid mechanics, arterial disease, and gene expression. *Annu Rev Fluid Mech*. 2014;46: 591–614.
10. Katranas SA, Kelekis AL, Antoniadis AP, Ziakas AG, Giannoglou GD. Differences in stress forces and geometry between left and right coronary artery: a pathophysiological aspect of atherosclerosis heterogeneity. *Hellenic J Cardiol*. 2015;56:217–223.
11. Lee J, Packard RR, Hsiao TK. Blood flow modulation of vascular dynamics. *Curr Opin Lipidol*. 2015;26:376–383.
12. Wentzel JJ, Chatzizisis YS, Gijssen FJ, Giannoglou GD, Feldman CL, Stone PH. Endothelial shear stress in the evolution of coronary atherosclerotic plaque and vascular remodelling: current understanding and remaining questions. *Cardiovasc Res*. 2012;96:234–243.
13. Chatzizisis YS, Coskun AU, Jonas M, Edelman ER, Feldman CL, Stone PH. Role of endothelial shear stress in the natural history of coronary atherosclerosis and vascular remodeling: molecular, cellular, and vascular behavior. *J Am Coll Cardiol*. 2007;49: 2379–2393.
14. Stone PH, Coskun AU, Yeghiazarians Y, et al. Prediction of sites of coronary atherosclerosis progression: In vivo profiling of endothelial shear stress, lumen, and outer vessel wall characteristics to predict vascular behavior. *Curr Opin Cardiol*. 2003;18:458–470.
15. Libby P, Ridker PM, Hansson GK. Progress and challenges in translating the biology of atherosclerosis. *Nature*. 2011;473: 317–325.

16. Wang C, Baker BM, Chen CS, Schwartz MA. Endothelial cell sensing of flow direction. *Arterioscler Thromb Vasc Biol.* 2013; 33:2130–2136.
17. Conway DE, Schwartz MA. Flow-dependent cellular mechano-transduction in atherosclerosis. *J Cell Sci.* 2013;126: 5101–5109.
18. Zhou J, Li YS, Chien S. Shear stress-initiated signaling and its regulation of endothelial function. *Arterioscler Thromb Vasc Biol.* 2014;34:2191–2198.
19. Siasos G, Tousoulis D, Siasou Z, Stefanadis C, Papavassiliou AG. Shear stress, protein kinases and atherosclerosis. *Curr Med Chem.* 2007;14:1567–1572.
20. Xu Q. Disturbed flow-enhanced endothelial turnover in atherosclerosis. *Trends Cardiovasc Med.* 2009;19:191–195.
21. Chien S. Molecular and mechanical bases of focal lipid accumulation in arterial wall. *Prog Biophys Mol Biol.* 2003;83: 131–151.
22. Himborg HA, Grzybowski DM, Hazel AL, LaMack JA, Li XM, Friedman MH. Spatial comparison between wall shear stress measures and porcine arterial endothelial permeability. *Am J Physiol Heart Circ Physiol.* 2004;286:H1916–H1922.
23. Johnson JL. Emerging regulators of vascular smooth muscle cell function in the development and progression of atherosclerosis. *Cardiovasc Res.* 2014;103:452–460.
24. Bryan MT, Duckles H, Feng S, et al. Mechanoresponsive networks controlling vascular inflammation. *Arterioscler Thromb Vasc Biol.* 2014;34:2199–2205.
25. Raaz U, Toh R, Maegdefessel L, et al. Hemodynamic regulation of reactive oxygen species: implications for vascular diseases. *Antioxid Redox Signal.* 2014;20:914–928.
26. Lam CF, Peterson TE, Richardson DM, et al. Increased blood flow causes coordinated upregulation of arterial eNOS and biosynthesis of tetrahydrobiopterin. *Am J Physiol Heart Circ Physiol.* 2006;290:H786–H793.
27. Go YM, Levonen AL, Moellering D, et al. Endothelial NOS-dependent activation of c-Jun NH(2)- terminal kinase by oxidized low-density lipoprotein. *Am J Physiol Heart Circ Physiol.* 2001;281:H2705–H2713.
28. Cheng C, Tempel D, van Haperen R, et al. Atherosclerotic lesion size and vulnerability are determined by patterns of fluid shear stress. *Circulation.* 2006;113:2744–2753.
29. Koskinas KC, Sukhova GK, Baker AB, et al. Thin-capped atheromata with reduced collagen content in pigs develop in coronary arterial regions exposed to persistently low endothelial shear stress. *Arterioscler Thromb Vasc Biol.* 2013;33: 1494–1504.
30. Hohberg M, Knochel J, Hoffmann CJ, et al. Expression of ADAMTS1 in endothelial cells is induced by shear stress and suppressed in sprouting capillaries. *J Cell Physiol.* 2011;226: 350–361.
31. Chu TJ, Peters DG. Serial analysis of the vascular endothelial transcriptome under static and shear stress conditions. *Physiol Genomics.* 2008;34:185–192.
32. Tousoulis D, Papageorgiou N, Syretos A, Stefanadis C. Assessing vulnerable plaque: is shear stress enough? *Int J Cardiol.* 2014; 172:e135–e138.
33. Chatzizisis YS, Baker AB, Sukhova GK, et al. Augmented expression and activity of extracellular matrix-degrading enzymes in regions of low endothelial shear stress colocalize with coronary atheromata with thin fibrous caps in pigs. *Circulation.* 2011;123:621–630.
34. Koskinas KC, Feldman CL, Chatzizisis YS, et al. Natural history of experimental coronary atherosclerosis and vascular remodeling in relation to endothelial shear stress: a serial, in vivo intravascular ultrasound study. *Circulation.* 2010;121:2092–2101.
35. Moreno PR, Falk E, Palacios IF, Newell JB, Fuster V, Fallon JT. Macrophage infiltration in acute coronary syndromes. Implications for plaque rupture. *Circulation.* 1994;90:775–778.
36. Quillard T, Araujo HA, Franck G, Shvartz E, Sukhova G, Libby P. TLR2 and neutrophils potentiate endothelial stress, apoptosis and detachment: implications for superficial erosion. *Eur Heart J.* 2015;36:1394–1404.
37. Cicha I, Worner A, Urschel K, et al. Carotid plaque vulnerability: a positive feedback between hemodynamic and biochemical mechanisms. *Stroke.* 2011;42:3502–3510.
38. Toutouzas K, Benetos G, Karanasos A, Chatzizisis YS, Giannopoulos AA, Tousoulis D. Vulnerable plaque imaging: updates on new pathobiological mechanisms. *Eur Heart J.* 2015.
39. Arbab-Zadeh A, Fuster V. The myth of the "vulnerable plaque": transitioning from a focus on individual lesions to atherosclerotic disease burden for coronary artery disease risk assessment. *J Am Coll Cardiol.* 2015;65:846–855.
40. Coskun AU, Yegiazarians Y, Kinlay S, et al. Reproducibility of coronary lumen, plaque, and vessel wall reconstruction and of endothelial shear stress measurements *in vivo* in humans. *Catheter Cardiovasc Interv.* 2003;60:67–78.
41. Bourantas CV, Papafaklis MI, Athanasiou L, et al. A new methodology for accurate 3-dimensional coronary artery reconstruction using routine intravascular ultrasound and angiographic data: implications for widespread assessment of endothelial shear stress in humans. *EuroIntervention.* 2013;9: 582–593.
42. Kern MJ, Moore JA, Aguirre FV, et al. Determination of angiographic (TIMI grade) blood flow by intracoronary Doppler flow velocity during acute myocardial infarction. *Circulation.* 1996; 94:1545–1552.
43. Papafaklis MI, Michalis LK. The effect of shear stress on the onset and progression of atheromatous disease and on restenosis following transluminal therapies. *Hellenic J Cardiol.* 2005;46:183–187.
44. Goubergrits L, Wellnhofer E, Kertzscher U, Affeld K, Petz C, Hege HC. Coronary artery WSS profiling using a geometry reconstruction based on biplane angiography. *Ann Biomed Eng.* 2009;37:682–691.
45. Tu S, Huang Z, Koning G, Cui K, Reiber JH. A novel three-dimensional quantitative coronary angiography system: *in-vivo* comparison with intravascular ultrasound for assessing arterial segment length. *Catheter Cardiovasc Interv.* 2010;76: 291–298.
46. Toutouzas K, Chatzizisis YS, Riga M, et al. Accurate and reproducible reconstruction of coronary arteries and endothelial shear stress calculation using 3D OCT: comparative study to 3D IVUS and 3D QCA. *Atherosclerosis.* 2015;240:510–519.
47. Lee JB, Chang SG, Kim SY, et al. Assessment of three dimensional quantitative coronary analysis by using rotational angiography for measurement of vessel length and diameter. *Int J Cardiovasc Imaging.* 2012;28:1627–1634.
48. Thim T, Hagensen MK, Wallace-Bradley D, et al. Unreliable assessment of necrotic core by virtual histology intravascular ultrasound in porcine coronary artery disease. *Circ Cardiovasc Imaging.* 2010;3:384–391.
49. Nair A, Margolis MP, Kuban BD, Vince DG. Automated coronary plaque characterisation with intravascular ultrasound backscatter: ex vivo validation. *EuroIntervention.* 2007;3:113–120.
50. Papafaklis MI, Bourantas CV, Yonetzu T, et al. Anatomically correct three-dimensional coronary artery reconstruction using frequency domain optical coherence tomographic and angiographic data: head-to-head comparison with intravascular ultrasound for endothelial shear stress assessment in humans. *EuroIntervention.* 2015;11:407–415.
51. Tu S, Holm NR, Christiansen EH, Reiber JH. First presentation of 3-dimensional reconstruction and centerline-guided assessment of coronary bifurcation by fusion of X-ray angiography and optical coherence tomography. *JACC Cardiovasc Interv.* 2012;5:884–885.

52. Li BH, Leung AS, Soong A, et al. Hybrid intravascular ultrasound and optical coherence tomography catheter for imaging of coronary atherosclerosis. *Catheter Cardiovasc Interv.* 2013;81:494–507.
53. Gardner CM, Tan H, Hull EL, et al. Detection of lipid core coronary plaques in autopsy specimens with a novel catheter-based near-infrared spectroscopy system. *JACC Cardiovasc Imaging.* 2008;1:638–648.
54. Pu J, Mintz GS, Brilakis ES, et al. In vivo characterization of coronary plaques: novel findings from comparing greyscale and virtual histology intravascular ultrasound and near-infrared spectroscopy. *Eur Heart J.* 2012;33:372–383.
55. Kang SJ, Mintz GS, Pu J, et al. Combined IVUS and NIRS detection of fibroatheromas: histopathological validation in human coronary arteries. *JACC Cardiovasc Imaging.* 2015;8:184–194.
56. Fard AM, Vacas-Jacques P, Hamidi E, et al. Optical coherence tomography—near infrared spectroscopy system and catheter for intravascular imaging. *Opt Express.* 2013;21:30849–30858.
57. Roleder T, Kovacic JC, Ali Z, et al. Combined NIRS and IVUS imaging detects vulnerable plaque using a single catheter system: a head-to-head comparison with OCT. *Euro-Intervention.* 2014;10:303–311.
58. Abran M, Stahli BE, Merlet N, et al. Validating a bimodal intravascular ultrasound (IVUS) and near-infrared fluorescence (NIRF) catheter for atherosclerotic plaque detection in rabbits. *Biomed Opt Express.* 2015;6:3989–3999.
59. Dixon AJ, Hossack JA. Intravascular near-infrared fluorescence catheter with ultrasound guidance and blood attenuation correction. *J Biomed Opt.* 2013;18:56009.
60. Ughi GJ, Verjans J, Fard AM, et al. Dual modality intravascular optical coherence tomography (OCT) and near-infrared fluorescence (NIRF) imaging: a fully automated algorithm for the distance-calibration of NIRF signal intensity for quantitative molecular imaging. *Int J Cardiovasc Imaging.* 2015;31:259–268.
61. Lee S, Lee MW, Cho HS, et al. Fully integrated high-speed intravascular optical coherence tomography/near-infrared fluorescence structural/molecular imaging in vivo using a clinically available near-infrared fluorescence-emitting indocyanine green to detect inflamed lipid-rich atheromata in coronary-sized vessels. *Circ Cardiovasc Interv.* 2014;7:560–569.
62. Ramkumar PG, Mitsouras D, Feldman CL, Stone PH, Rybicki FJ. New advances in cardiac computed tomography. *Curr Opin Cardiol.* 2009;24:596–603.
63. Frauenfelder T, Boutsianis E, Schertler T, et al. In-vivo flow simulation in coronary arteries based on computed tomography datasets: feasibility and initial results. *Eur Radiol.* 2007;17:1291–1300.
64. Hetterich H, Jaber A, Gehring M, et al. Coronary computed tomography angiography based assessment of endothelial shear stress and its association with atherosclerotic plaque distribution in-vivo. *PLoS One.* 2015;10:e0115408.
65. Choi G, Lee JM, Kim HJ, et al. Coronary artery axial plaque stress and its relationship with lesion geometry: application of computational fluid dynamics to coronary CT angiography. *JACC Cardiovasc Imaging.* 2015.
66. Katranas SA, Kelekis AL, Antoniadis AP, Chatzizisis YS, Giannoglou GD. Association of remodeling with endothelial shear stress, plaque elasticity, and volume in coronary arteries: a pilot coronary computed tomography angiography study. *Angiology.* 2014;65:413–419.
67. Gijsen FJ, Schuurbiers JC, van de Giessen AG, Schaap M, van der Steen AF, Wentzel JJ. 3D reconstruction techniques of human coronary bifurcations for shear stress computations. *J Biomech.* 2014;47:39–43.
68. Achenbach S. Can CT detect the vulnerable coronary plaque? *Int J Cardiovasc Imaging.* 2008;24:311–312.
69. Maurovich-Horvat P, Ferencik M, Voros S, Merkely B, Hoffmann U. Comprehensive plaque assessment by coronary CT angiography. *Nat Rev Cardiol.* 2014;11:390–402.
70. van der Giessen AG, Gijsen FJ, Wentzel JJ, et al. Small coronary calcifications are not detectable by 64-slice contrast enhanced computed tomography. *Int J Cardiovasc Imaging.* 2011;27:143–152.
71. Oberoi S, Meinel FG, Schoepf UJ, et al. Reproducibility of noncalcified coronary artery plaque burden quantification from coronary CT angiography across different image analysis platforms. *AJR Am J Roentgenol.* 2014;202:W43–W49.
72. Pedrigi RM, Poulsen CB, Mehta JV, et al. Inducing persistent flow disturbances accelerates atherogenesis and promotes thin cap fibroatheroma development in D374Y-PCSK9 hypercholesterolemic minipigs. *Circulation.* 2015;132:1003–1012.
73. Koskinas KC, Chatzizisis YS, Papafaklis MI, et al. Synergistic effect of local endothelial shear stress and systemic hypercholesterolemia on coronary atherosclerotic plaque progression and composition in pigs. *Int J Cardiol.* 2013;169:394–401.
74. Stone PH, Coskun AU, Kinlay S, et al. Regions of low endothelial shear stress are the sites where coronary plaque progresses and vascular remodelling occurs in humans: an in vivo serial study. *Eur Heart J.* 2007;28:705–710.
75. Stone PH, Coskun AU, Kinlay S, et al. Effect of endothelial shear stress on the progression of coronary artery disease, vascular remodeling, and in-stent restenosis in humans: in vivo 6-month follow-up study. *Circulation.* 2003;108:438–444.
76. Corban MT, Eshtehardi P, Suo J, et al. Combination of plaque burden, wall shear stress, and plaque phenotype has incremental value for prediction of coronary atherosclerotic plaque progression and vulnerability. *Atherosclerosis.* 2014;232:271–276.
77. Eshtehardi P, McDaniel MC, Suo J, et al. Association of coronary wall shear stress with atherosclerotic plaque burden, composition, and distribution in patients with coronary artery disease. *J Am Heart Assoc.* 2012;1:e002543.
78. Samady H, Eshtehardi P, McDaniel MC, et al. Coronary artery wall shear stress is associated with progression and transformation of atherosclerotic plaque and arterial remodeling in patients with coronary artery disease. *Circulation.* 2011;124:779–788.
79. Papafaklis MI, Mizuno S, Takahashi S, et al. Incremental predictive value of combined endothelial shear stress, plaque necrotic core, and plaque burden for future cardiac events: a post-hoc analysis of the PREDICTION study. *Int J Cardiol.* 2015;202:64–66.
80. Ueshima H, Sekikawa A, Miura K, et al. Cardiovascular disease and risk factors in Asia: a selected review. *Circulation.* 2008;118:2702–2709.
81. Stone PH, Saito S, Takahashi S, et al. Prediction of progression of coronary artery disease and clinical outcomes using vascular profiling of endothelial shear stress and arterial plaque characteristics: the PREDICTION Study. *Circulation.* 2012;126:172–181.
82. Stone GW, Maehara A, Lansky AJ, et al. A prospective natural-history study of coronary atherosclerosis. *N Engl J Med.* 2011;364:226–235.
83. Stone PHMA, Coskun AU, Maynard C, Andreou I, Siasos G, Local Low Endothelial Shear Stress (ESS) Provides Incremental Prediction of Non-culprit MACE in Addition to Plaque Burden, Minimal Lumen Area, and Plaque Morphology: The PROSPECT Study. *Transcatheter Cardiovascular Therapeutics.* San Francisco: J Am Coll Cardiol; 2015.
84. Kubo T, Maehara A, Mintz GS, et al. The dynamic nature of coronary artery lesion morphology assessed by serial virtual

- histology intravascular ultrasound tissue characterization. *J Am Coll Cardiol.* 2010;55:1590–1597.
85. Vergallo R, Papafakis MI, Yonetsu T, et al. Endothelial shear stress and coronary plaque characteristics in humans: combined frequency-domain optical coherence tomography and computational fluid dynamics study. *Circ Cardiovasc Imaging.* 2014;7:905–911.
86. Otsuka F, Finn AV, Yazdani SK, Nakano M, Kolodgie FD, Virmani R. The importance of the endothelium in atherosclerosis and coronary stenting. *Nat Rev Cardiol.* 2012;9:439–453.
87. Bourantas CV, Papafakis MI, Kotsia A, et al. Effect of the endothelial shear stress patterns on neointimal proliferation following drug-eluting bioresorbable vascular scaffold implantation: an optical coherence tomography study. *JACC Cardiovasc Interv.* 2014;7:315–324.
88. Wentzel JJ, Krams R, Schoubiers JC, et al. Relationship between neointimal thickness and shear stress after Wallstent implantation in human coronary arteries. *Circulation.* 2001;103:1740–1745.
89. Bourantas CV, Raber L, Zaugg S, et al. Impact of local endothelial shear stress on neointima and plaque following stent implantation in patients with ST-elevation myocardial infarction: a subgroup-analysis of the COMFORTABLE AMI-IBIS 4 trial. *Int J Cardiol.* 2015;186:178–185.
90. Papafakis MI, Bourantas CV, Theodorakis PE, et al. The effect of shear stress on neointimal response following sirolimus- and paclitaxel-eluting stent implantation compared with bare-metal stents in humans. *JACC Cardiovasc Interv.* 2010;3:1181–1189.
91. Bourantas CV, Papafakis MI, Lakkas L, et al. Fusion of optical coherence tomographic and angiographic data for more accurate evaluation of the endothelial shear stress patterns and neointimal distribution after bioresorbable scaffold implantation: comparison with intravascular ultrasound-derived reconstructions. *Int J Cardiovasc Imaging.* 2014;30:485–494.
92. Bourantas CV, Garcia-Garcia HM, Naka KK, et al. Hybrid intravascular imaging: current applications and prospective potential in the study of coronary atherosclerosis. *J Am Coll Cardiol.* 2013;61:1369–1378.
93. Chatzizisis YS, Jonas M, Beigel R, et al. Attenuation of inflammation and expansive remodeling by Valsartan alone or in combination with Simvastatin in high-risk coronary atherosclerotic plaques. *Atherosclerosis.* 2009;203:387–394.
94. Takahashi S, Papafakis MI, Sakamoto S, et al. The effect of statins on high-risk atherosclerotic plaque associated with low endothelial shear stress. *Curr Opin Lipidol.* 2011;22:358–364.
95. Liang C, Xiaonan L, Xiaojun C, et al. Effect of metoprolol on vulnerable plaque in rabbits by changing shear stress around plaque and reducing inflammation. *Eur J Pharmacol.* 2009;613:79–85.
96. Holme MN, Fedotenko IA, Abegg D, et al. Shear-stress sensitive lenticular vesicles for targeted drug delivery. *Nat Nanotechnol.* 2012;7:536–543.